PAPER • OPEN ACCESS

Novel Simplified Blade Hub Line Optimization of High-Pressure Ratio Centrifugal Compressor Design Using Numerical Simulations

To cite this article: A Khan *et al* 2020 *IOP Conf. Ser.: Mater. Sci. Eng.* **899** 012010

IOP Conf. Series: Materials Science and Engineering **899** (2020) 012010 doi:10.1088/1757-899X/899/1/012010

Novel Simplified Blade Hub Line Optimization of High-Pressure Ratio Centrifugal Compressor Design Using Numerical Simulations

A Khan[1*], F Ahmad[2], S Ali[1], M R Siddiqi[1] and M Z Ijaz[1]

[1]Department of Mechanical Engineering, CECOS University of IT and Emerging Sciences, Peshawar, Pakistan
[2]Department of Mechanical and Aerospace Engineering, Air University, Islamabad, Pakistan

[1*]E-mail: amjid@cecos.edu.pk

Abstract. The focus of this research is to numerically investigate the effect of blade hub line variation on the performance (Total pressure-ratio and Isentropic-Efficiency) of centrifugal compressor from stall to choke to study the operating range and stall margin. An optimization technique is carried out in which the meridional profile hub line is modified and compared with the high Mach number SRV2 compressor designed and fabricated by DLR (German Aerospace Center). Numerical simulations showed significant increase in the stall margin and operating range by bargaining on pressure ratio and isentropic efficiency. Reynolds Averaged Navier Stokes (RANS) based k-ε model is used to predict turbulence using numerical simulations. The value of Y plus for the structured mesh near the boundaries is kept 35. Blade hub line being the important parameter, has substantial performance improvement of centrifugal compressor. The novel design improved the stall margin by 44 percent while operating range from stall to choke has been upgraded by 7.5 percent.

1. Introduction

A mechanical device used to increase the total pressure of a ideal air fluid is called centrifugal compressor. Applications of centrifugal compression systems include gas turbine engines, turbochargers, powering tanks and rotorcraft, chemical industries, compression and transportation of hydrogen in petrochemical refineries, and refrigeration systems. Centrifugal compressors are used for low-flow rate applications because it has higher pressure ratio to weight ratio as compared to axial compression systems [1].

Optimization technique in the meridional profile is one of the important parameters in selection of centrifugal compressors for the specific applications [2]. When high pressure rise at low mass flow rate is desired, centrifugal compressor is considered for such applications [3]. For turbochargers, centrifugal compressors with high operating range and high stall margin is desired [4]. Hideo Nishida et al. investigated the blade loading optimization by increasing the back-sweep angle. This increase in the back-sweep angle is used to suppress the reduction in the surge margin and test results showed that the isentropic efficiency has been increased by 5% compared with the standard design [5]. For turbochargers applications, centrifugal compressors with high stall margin is required but at low mass flow rate flow instabilities leads to high aerodynamic loss and structural damage [6]. These flow instabilities are stall and surge [7]. The flow separation and flow recirculation due to adverse pressure gradient is called stall and surge is divided into two types i.e. mild surge and deep surge depending on the flow fluctuation and back flow condition [8].

Different optimization techniques have been carried out to improve the performance of the centrifugal compressor. Tip clearance optimization is carried out to observe its effect on the pressure ratio and efficiency of the compressor. At constant tip clearance of 0.1mm highest pressure ratio and efficiency is found [9]. Amjid et al. numerically investigated the influence of diffuser exit width on the performance of centrifugal compressor and it is found that increasing the diffuser exit decreases the pressure ratio and efficiency due to increase of entropy generation at the outlet of the impeller [10].

C. Xu and Amano studied the meridional impacts of the centrifugal compressor and they found that changing the meridional profile one way or another, it affects the performance of the compressor [11]. The study further shows that a proper meridional profile can improve overall performance of centrifugal compressor and reduce the sensitivity of the tip clearance [12]. T. Raitor et al. studied the geometry optimization of the impeller blade with 45 free parameters. The optimized design of the impeller improved the efficiency by 1.9 percent and operating range was also increased significantly. The forward sweep angle of the blade reduced the shock losses at the leading edge of the impeller [13]. Hong Xie et al. modified the meridional plane for the high operating range and efficient design and results showed that by changing the meridional profile of the compressor greatly effects the performance of the centrifugal compressor by increasing the stall margin and efficiency [2]. Amjid et al. numerically studied the effect of varying meridional profile and thickness and they concluded that increasing back-sweep angle at the leading edge increases the stall margin by 0.8%, optimizing the blade angle at the trailing edge increases the stall margin by 1.1% and increasing the thickness of the blade increases the stall margin by 0.2% [4].

1.1. Specifications of Test Case Compressor

A centrifugal compressor test case having high pressure ratio, mass flow coefficient and specific speed has been studied to understand effect of varying meridional profile, blade angles and thickness. The test case was designed and built by DLR (German Aerospace Center). The basic geometric parameters have been documented in Table 1.

As shown in the Fig. 2, impeller with13 full and 13 splitter blades. Splitter blades leading edges is at 26% of full blade chord. The exit diameter of test case compressor is 112 mm and nominal tip speed is 586 m/s at 50000 1/min. A vaneless diffuser is connected after the impeller [14].

The compressor (SRV2-O) test case data is shown in table:

Table I: Specifications of Test Case Compressor

Parameter	**Value**	**Units**
Inlet ambient pressure, P_{t1}	101325	[Pa]
Inlet ambient temperature, T_{t1}	288.15	[K]
Design Shaft speed, n	50000	[1/min]
Design mass flow rate, m	2.55	[kg/s]
Number of full/splitter blades	13/13	-
Tip speed of Impeller	586	[m/s]
Pressure ratio of Impeller	6.1	-
Impeller efficiency	84%	-

2. Numerical Setup

For CFD model to acquire, a step by step methodology has been taken on for numerical simulations. The model development consists of following steps such as Geometric parameterization in BladeGen, Computational method for meshing in TurboGrid, Computational solver, Turbulence model and boundary conditions in ANSYS CFX.

2.1. Governing Equations

The succeeding postulates based on the theoretical background are considered to shape a three-dimensional fluid flow model using a cartesian co-ordinate system [15]:

1) The presided flow is considered as continuum, and a no slip boundary condition is valid
2) The flow is compressible ideal flow
3) The flow is studied as turbulent because of high Reynolds number of 3.65×10^6
4) A steady-state fluid flow is considered
5) The compressor walls are considered as completely smooth
6) The viscous dissipation effect is considered in the energy equations as it is very important in case of compressor to study viscous sublayer for flow separation
7) Compressor stage geometry is same as experimental setup
8) Turbulence model is K- ε model
9) Design mass flow rate 2.55kg/s
10) Design speed of 50,000 1/min

Based on postulates, a mathematical model is designed using the following equations [15]:

Continuity Equation:

$$\frac{\partial u}{\partial x}+\frac{\partial v}{\partial y}+\frac{\partial w}{\partial z}=0 \tag{1}$$

Where u, v and w are the velocity components and x, y and z are cartesian co-ordinates.

Momentum Equation:

In the x-direction,

$$u\frac{\partial u}{\partial x}+v\frac{\partial u}{\partial y}+w\frac{\partial u}{\partial z}=-\frac{1}{\rho_f}\frac{\partial p}{\partial x}+\frac{\mu_f}{\rho_f}\left(\frac{\partial^2 u}{\partial x^2}+\frac{\partial^2 u}{\partial y^2}+\frac{\partial^2 u}{\partial z^2}\right) \tag{2}$$

In the y-direction,

$$u\frac{\partial v}{\partial x}+v\frac{\partial v}{\partial y}+w\frac{\partial v}{\partial z}=-\frac{1}{\rho_f}\frac{\partial p}{\partial y}+\frac{\mu_f}{\rho_f}\left(\frac{\partial^2 v}{\partial x^2}+\frac{\partial^2 v}{\partial y^2}+\frac{\partial^2 v}{\partial z^2}\right) \tag{3}$$

In the z-direction,

$$u\frac{\partial w}{\partial x}+v\frac{\partial w}{\partial y}+w\frac{\partial w}{\partial z}=-\frac{1}{\rho_f}\frac{\partial p}{\partial z}+\frac{\mu_f}{\rho_f}\left(\frac{\partial^2 w}{\partial x^2}+\frac{\partial^2 w}{\partial y^2}+\frac{\partial^2 w}{\partial z^2}\right) \tag{4}$$

where ρ_f and μ_f are density and dynamic viscosity of the working fluid, respectively. Note, that p stands for pressure.

Energy Equation:

$$u\frac{\partial T_f}{\partial x}+v\frac{\partial T_f}{\partial y}+w\frac{\partial T_f}{\partial z}=\frac{k_f}{\rho_f\, C_{pf}}\frac{\partial p}{\partial z}+\left(\frac{\partial^2 T_f}{\partial x^2}+\frac{\partial^2 T_f}{\partial y^2}+\frac{\partial^2 T_f}{\partial z^2}\right) \tag{5}$$

Where $C_{pf,}$ $k_{f\ ,}$ and T_f are the constant specific heat capacity, thermal conductivity and temperature of the working fluid.

One of the important parameters in centrifugal compressor is stall margin, which can be calculated using the equation:

$$stall\ margin = 1-\frac{\dot{m}_{stall}}{\dot{m}_{design}} \tag{6}$$

The total operating range for the performance map from stall to choke is calculated using the following equation:

$$Operating\ range = (\dot{m}_{choke}-\dot{m}_{stall})/\dot{m}_{choke} \tag{7}$$

The Performance analysis of centrifugal compressor stage is assessed by performance parameters i.e. isentropic efficiency and pressure ratio, from inlet duct of impeller to diffuser outlet. Pressure ratio is evaluated using below equation:

$$Pr = \left[\int P_d * \frac{dm^{\cdot}}{m^{\cdot}}\right] / P_0 \qquad (8)$$

Where P_d is the pressure at diffuser outlet, P_0 is pressure at inlet of compressor, $m^{\cdot}$ is the mass flow rate and Pr stands for total pressure ratio. Total to total isentropic efficiency can be found using Pr found in the above equation:

$$\eta_{tt} = T_i(Pr^{\frac{\gamma-1}{\gamma}} - 1)/(T_d - T_i) \qquad (9)$$

Where η_{tt} stands for total to total isentropic efficiency, T_i stands for inlet temperature and T_d stands for temperature at diffuser outlet.

2.2. *Geometric Parameterization in BladeGen*

The primary step in pre-processing is to acquire an accurate geometric model of the compressor. For the test case compressor under examination, data has been taken from the German Aerospace Centre (DLR) and this data has been 3D modelled in BladeGen. This tool allows quick definition of radial blade flows and gives an important link between blade design and simulations.

For the test case study, the inlet duct, impeller and diffuser have been modelled as single domain. Only single domain has been considered for numerical simulations to reduce computational efforts required for the simulations as shown in Fig 1.

2.3. *Computational Method for Meshing (Turbogrid)*

After modelling centrifugal compressor in BladeGen, an H-grid mesh topology was created in ANSYS TurboGrid module for the entire fluid domain i.e. Inlet duct, Impeller and diffuser. TurboGrid is a meshing scheme for turbomachinery configurations, it selects automatic and refined mesh quality for most complex geometries creating hexahedral structured mesh. To study viscous sublayer, a very refined mesh has been created near the wall by providing adequate number of nodes near the boundary layer. For the better mesh quality, compressor computational domain is divided to H-grid topology with splitter blades arrangement. Design tip clearance for this case is variable tip-clearance of 0.5 mm(at blade leading edge),0.3 mm(at blade trailing edge). Mesh is generated using H-grid with 25 number of elements at the inlet and outlet each. A grid independency test executed using 8 distinct grid sizes for complete compressor. The grid with total number of mesh elements 560788 and total number of nodes 504345, has been found adequate as alteration in pressure ratio and isentropic efficiency was negligible in this range of elements as shown in Fig. 1 [16].

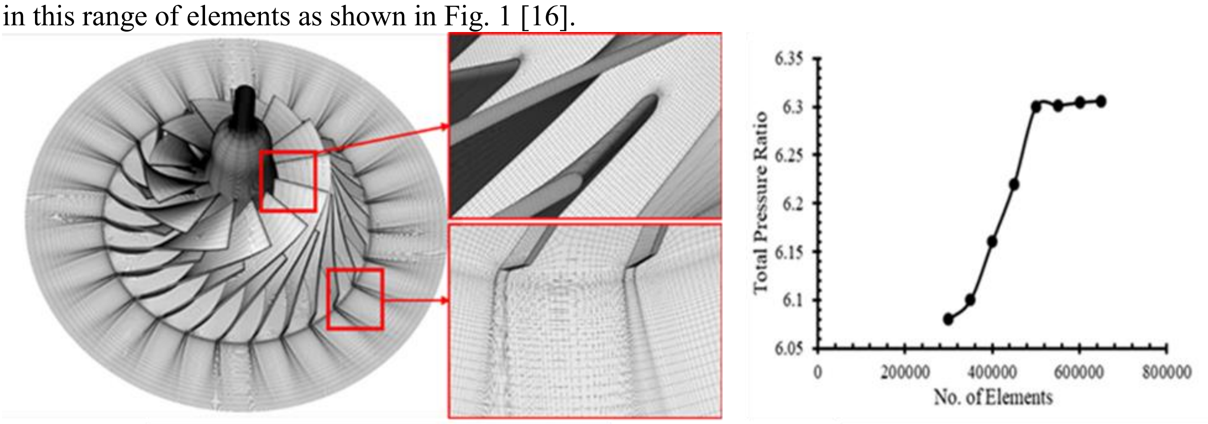

(a) Computational Mesh (TurboGrid) (b) Grid Independency Test

Figure 1: Computational Grid

IOP Conf. Series: Materials Science and Engineering **899** (2020) 012010 doi:10.1088/1757-899X/899/1/012010

2.4. Turbulence Model
For CFD simulations ANSYS CFX 15 was used to model the flow field for centrifugal compressor under steady state conditions. K-epsilon turbulence model is used for the numerical simulations. K-epsilon model gives better results for planar shear layer and recirculating flows as is the case of centrifugal compressor. According to the K-epsilon turbulence model criteria, the value of Y-plus is set 35.

2.5. Numerical Setup and Boundary Conditions
The compressor inlet conditions for all simulated cases.

$$T_i = 288.15\ k \tag{10}$$

$$P_i = 101.325\ kpa \tag{11}$$

$$Convergence\ Criteria = 1 * 10^{-5} \tag{13}$$

The medium turbulence intensity is kept 5% according to standard ambient conditions used by DLR (German Aerospace Center) for turbocharger configuration. The convergence criterion is set to the above mentioned value for all residuals while for monitoring convergence, mass flow rate and isentropic efficiency has been recorded for choke margin. As, at choke point minor variation in mass flow rate cause substantial variation in performance, so to check choke limit, static pressure is defined at outlet while mass flow rate is monitored, and choke point is found by slightly reducing static pressure at outlet [12]. The stage or mixing plane interfaces have been defined between diffuser, impeller and inlet. The rotational periodicity has been defined at boundaries of single passage assuming flow symmetry in all passages [17].

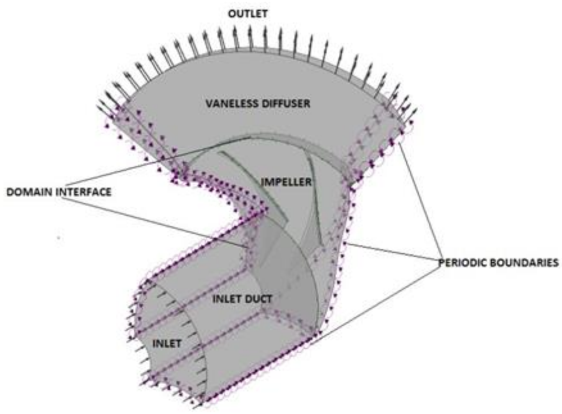

Figure 2: Computational Domain

2.6. Creating the Design Space
To study the effect of varying hub line, different design spaces have been created in the angle range of 40°-50° and the effect of the hub line variation has been analysed.

The impeller hub line has been modified using Bezier curve and analyzed its effect on the performance parameters of test case compressor as shown in Fig. 4. The new modified design has blade hub line adjusted at different angles from 40 to 50 degree, but the most optimized design has the angle adjusted at 45 degree as shown in Fig. 3. Bezier curves are used for describing the geometry of the curves.

$$p(t) = \sum_{i=0}^{n} ci\, B_i^n\ (t) \qquad t\epsilon[0,1] \tag{14}$$

Where ci represent control points and B_i^n represent ith Bernstein polynomial degree of n. To control the curve systematically, Bezier curves are used for this purpose. Which allow control of the

IOP Conf. Series: Materials Science and Engineering **899** (2020) 012010 doi:10.1088/1757-899X/899/1/012010

curve and the curve obtained by the help of continuous derivatives is smooth line. Control polygon is the name given to control lines between successive control points. Bezier curve passes through the control points and specifically through first and last point. So, in this research project, hub line has been adjusted using Bezier curve technique.

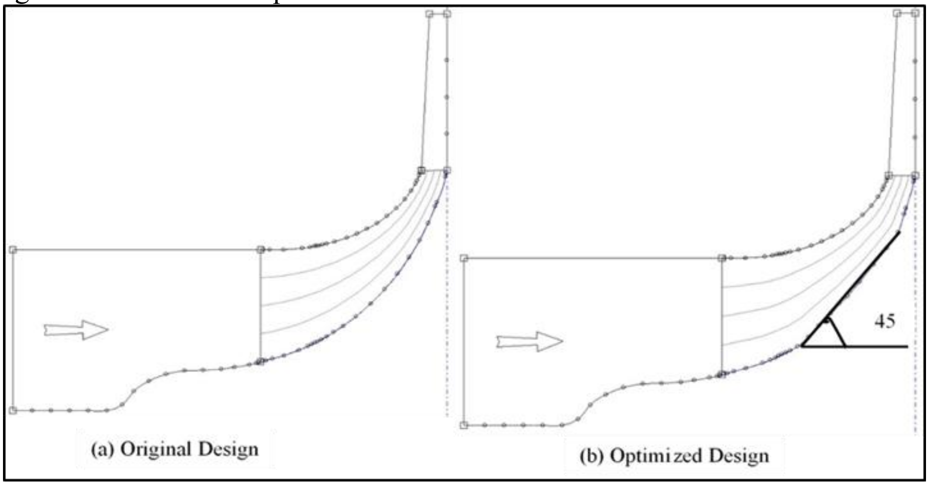

Figure 3: Design Space

3. Results and Discussions

3.1. Overall Performance

The overall performance of the compressor is analysed by making following agreements with the experimental test case:

- Design mass flow rate of 2.55kg/s
- Design speed of 50,000 rpm
- Turbulence model is k-ε model

Numerical simulations are carried out using ANSYS CFX solver at design conditions, total pressure ratio and total to total isentropic efficiency has been extracted from stall to choke to compare with the experimental data. The validation of the experimental data is carried out to show the suitability of this solver with the real-world problems. A very realistic results were shown by the simulated data as numerical simulations over predicted the experimental data by 9% only. Then numerical simulations are performed for the optimization of new compressor design as shown in Fig. 4. The optimization technique was performed by the hub line from 40° to 50° angle using Bezier Curve technique by keeping the rest of compressor same as experimental design. The analysis showed that hub line at angle of 45° angle shows the highest operating range and stall margin as shown in Fig. 3 and Fig. 4.

The operating range and stall margin for the experimental and numerically optimized design is calculated using equation 6 and 7. The operating range for experimental design is 16.9% while operating range for the CFD optimized design is found 18.18% from stall to choke. Hence, the total increase in the operating range for the optimized design is 7.5%. The stall margin for the experimental test margin is 5.7% while 8.24% for the optimized design. Hence, the percent increase in stall margin for the optimized design is 44% as shown in Fig. 4. All these compressors with high operating range and stall margin are used for the turbochargers applications to overcome the flow instabilities at low mass flow rate. The flow instabilities like flow recirculation and flow reversal due to adverse pressure gradient at low mass flow rate is called stall. The analysis only showed difference in the stall point, so the rest of analysis will be carried out at stall point to compare the experimental design and the CFD Optimized design.

IOP Conf. Series: Materials Science and Engineering **899** (2020) 012010 doi:10.1088/1757-899X/899/1/012010

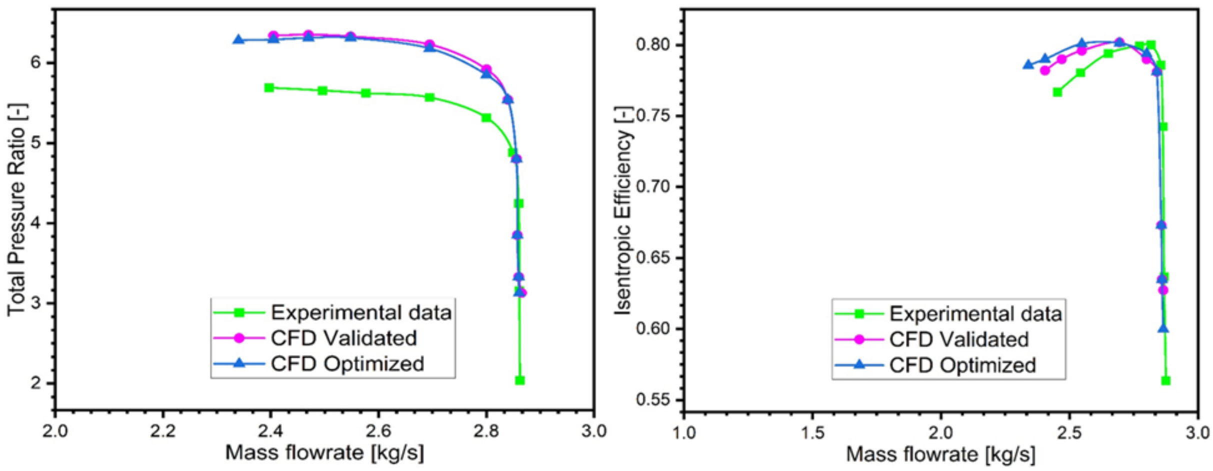

Figure 4: Performance Map

3.2. Diffuser Flow Separation

Factors that leads to centrifugal compressor instabilities are the flow separation and flow recirculation due to adverse pressure gradient, termed as Stall. These flow instabilities occur at low mass flowrate which leads to noise, vibration and sometimes fatal failure. In most of the cases flow separation occur at the trailing edge of the impeller blade and extends towards diffuser shroud, which has drastic effect on the compressor performance. These flow recirculation and flow separation effects is shown in Fig. 5, shown by the stagnant velocity contours and wakes at diffuser inlet. It is evident from the figure that these flow recirculation/wakes/jets are more obvious in the experimental design as compared to new optimized design. Which means that the new optimized design gives better performance to control flow instabilities and can be used in applications like turbochargers compressors.

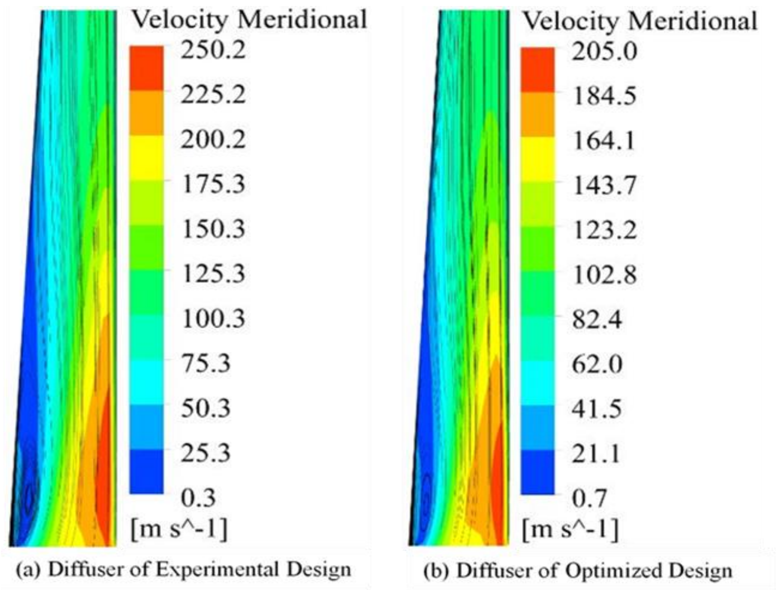

Figure 5: Diffuser Flow Separation

3.3. Entropy Generation

In Fig. 6 and Fig. 7, entropy generation for stall point from inlet to outlet of the impeller along the meridional plane has been drawn which shows that entropy generation for the optimized design is smaller as compared to experimental design. This means that losses in the optimized design has been significantly reduced, which occurs because of secondary flow due to tip leakages, flow separation and flow recirculation. Then, static entropy contours are drawn along meridional length normalized and analyzed the maximum entropy regions, it is evident from the figure that maximum losses region is the blade trailing edge and it is significantly reduced in case of optimized design.

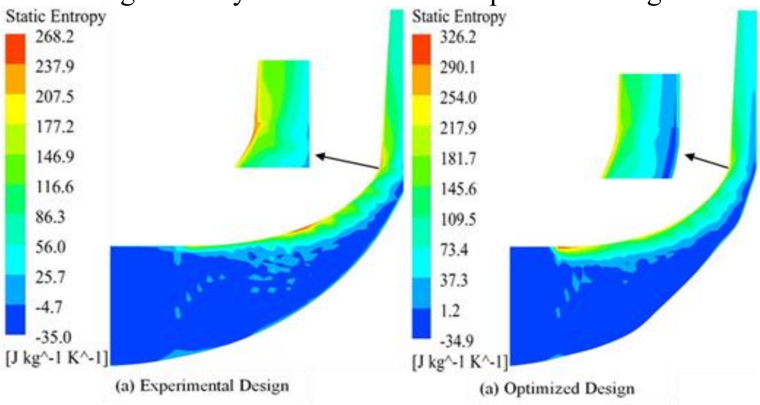

Figure 6: Entropy Generation from Inlet to Outlet of Impeller

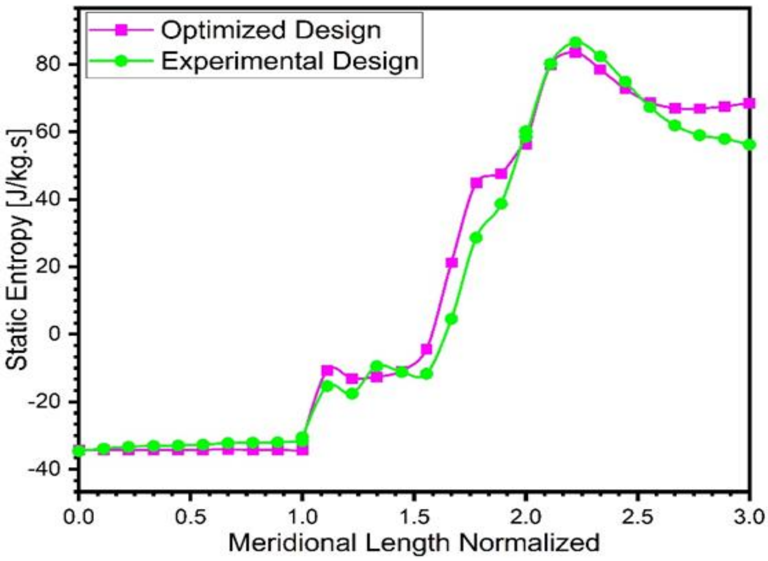

Figure 7: Entropy Generation from Inlet to Outlet of Impeller

3.4. Blade Loading

Blade loading represents the maximum load that is applied on the blade, which means that increasing blade loading causes more fatigue failure in case of centrifugal compressor. It is usually represented on the static pressure rise on each side of impeller blades (suction and pressure side). As it is evident from the Fig. 8, that blade loading for experimental design is higher as compared to optimized design for the same pressure ratio at stall point, which means that optimized design will have more fatigue life for the same application and same pressure ratio.

3.5. Meridional Velocity

Meridional velocity contours can be efficiently used to study the flow separation and shock waves generation in centrifugal compressor. It is clear from Fig. 9, that flow separation occurs at the diffuser shroud of the compressor and maximum velocity flow appears at impeller hub side. Meridional velocity is maximum at the hub line of the centrifugal compressor, which is reduced in the optimized design and as a result it reduces flow separation on the diffuser shroud. This means that tolerance capability for stall to control is maximum in optimized design. The figures indicate that at same pressure ratio and same efficiency, the optimized design will have small shock losses, small flow separation and low flow instabilities. So, the optimized design performance is much better than the experimental design while keeping meridional velocity, Mach number, total pressure ratio, isentropic efficiency and flow instabilities in view.

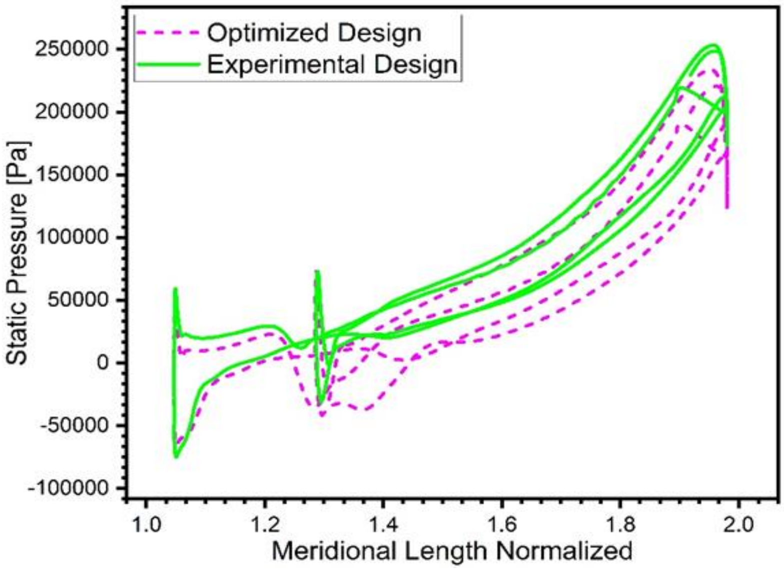

Figure 8: Blade Loading Diagram

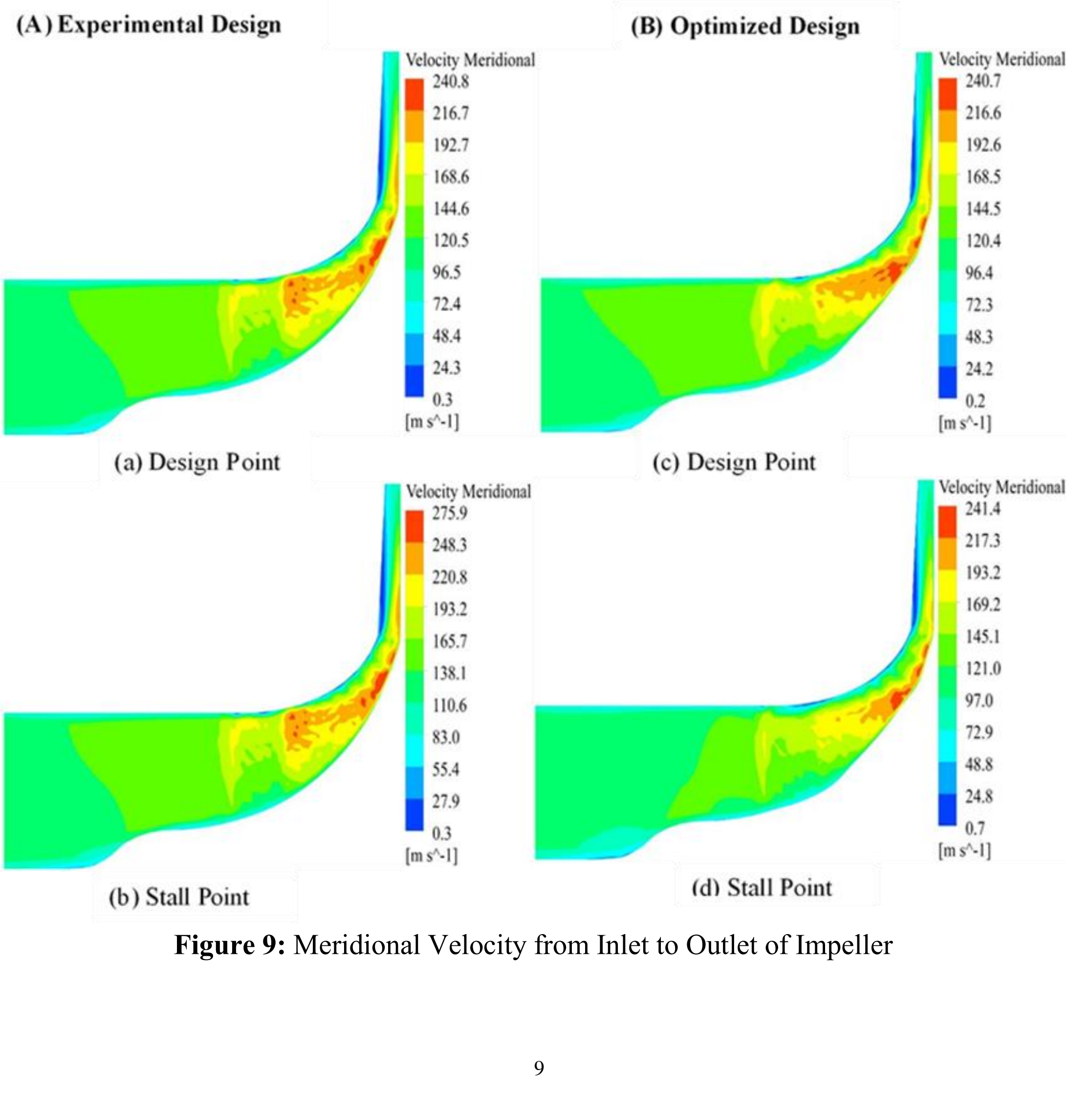

Figure 9: Meridional Velocity from Inlet to Outlet of Impeller

4. Conclusions

For the hub line optimization, 10 different designs have been analyzed by straitening the hub line from angle 40° to 50°. The 45° hub line is found the most optimized design with high operating range, stall margin, pressure ratio and isentropic efficiency. Based on detailed steady state computational fluid dynamics analysis, following conclusions can be drawn:

- As the hub line is straightened, made the impeller design much simpler. The simplified design results in low cost and low processing time
- Ansys CFX showed very realistic results by overpredicting the experimental data by 9% only
- By applying passive flow control method for flow instabilities, pressure ratio and efficiency decreases but in case of optimized design very slight reduction in pressure ratio and efficiency is found
- The operating range is increased by 7.5% while the stall margin is improved by 44% for the same operating conditions

Table II: Summary of Conclusions

Parameters	Experimental Design	Optimized Design
Operating Range (%)	16.9	18.18
Stall Margin (%)	5.7	8.24
Pressure Ratio	6.34	6.30
Isentropic Efficiency (%)	78	79

References

[1] A. R. Avio, “Aerodesign and Performance Analysis of a Radial Transonic Impeller for a 9 : 1 Pressure Ratio Compressor,” vol. 115, no. July 1993, pp. 573–581, 2017.
[2] H. Xie, M. Song, X. Liu, B. Yang, and C. Gu, “Research on the Simplified Design of a Centrifugal Compressor Impeller Based on Meridional Plane Modification,” *Appl. Sci.*, vol. 8, no. 8, p. 1339, 2018.
[3] C. Compressors, “Lesson 21,” *Comp. A J. Comp. Educ.*, pp. 1–26.
[4] T. Ullah *et al.*, “Blade Meridional Profile Optimization for Novel High-Pressure Ratio Centrifugal Compressor Design Using Numerical Simulations,” 2020.
[5] T. Shibata, M. Yagi, H. Nishida, H. Kobayashi, and M. Tanaka, “Performance improvement of a centrifugal compressor stage by increasing degree of reaction and optimizing blade loading of a 3D-impeller,” *Proc. ASME Turbo Expo*, vol. 7, no. PART B, pp. 1305–1315, 2009.
[6] X. Xue, T. Wang, T. Zhang, and B. Yang, “Mechanism of stall and surge in a centrifugal compressor with a variable vaned diffuser,” *Chinese J. Aeronaut.*, vol. 31, no. 6, pp. 1222–1231, 2018.
[7] A. Khan, M. U. Siddiqi, and F. Ahmad, “Numerical Investigation of Transonic High-Pressure Ratio Centrifugal Compressor,” vol. 16, no. 2, pp. 83–95, 2020.
[8] A. Stein, S. Niazi, and L. N. Sankar, “Computational Analysis of Stall and Separation Control in Centrifugal Compressors Introduction,” vol. 16, no. 1, 2000.
[9] A. Khan and A. Javed, “Performance Variation of Transonic Centrifugal Compressor at Different Tip Clearances Using Numerical Simulations,” pp. 2–7.
[10] A. Khan and T. Ullah, “Numerical Analysis of Flow through High Pressure Ratio Centrifugal Compressor Impeller and Effect of varying Diffuser Exit Width on Performance,” vol. 6, no. 11, pp. 399–405, 2019.
[11] C. Xu and R. S. Amano, “Meridional considerations of the centrifugal compressor development,” *Int. J. Rotating Mach.*, vol. 2012, 2012.

[12] A. Javed and E. Kamphues, "Evaluation of the Influence of Volute Roughness on Turbocharger Compressor Performance From a Manufacturing Perspective," p. V02DT42A040, 2014.
[13] T. Raitor, O. Reutter, M. Aulich, and E. Nicke, "Aerodynamic design studies of a transonic centrifugal compressor impeller based on automated 3D-CFD optimization," *10th Eur. Conf. Turbomach. Fluid Dyn. Thermodyn. ETC 2013*, pp. 809–819, 2014.
[14] G. Eisenlohr, P. Dalbert, H. Krain, H. Pröll, F.-A. Richter, and K.-H. Rohne, "Analysis of the Transonic Flow at the Inlet of a High Pressure Ratio Centrifugal Impeller," p. V001T01A007, 2014.
[15] M. M. U. Rehman, T. A. Cheema, F. Ahmad, M. Khan, and A. Abbas, "Thermodynamic Assessment of Microchannel Heat Sinks with Novel Sidewall Ribs," pp. 1–12, 1981.
[16] P. Kapoor, "Influence of Surface Roughness on Flow Instabilities in a Centrifugal Compressor," pp. 1–24.
[17] F. Ghigliazza, A. Traverso, M. L. Ferrari, and J. Wingate, "Gt2008-50562," *Asme Gt*, pp. 1–9, 2008.